Gas-phase rate coefficient of OH + cyclohexene oxide measured from 251 to 373 K

Hajar El Othmani, Yangang Ren, Wahid Mellouki, Véronique Daële, Max Mcgillen

1   **Gas-phase rate coefficient of OH + cyclohexene oxide measured from 251–373 K**

2   **Author list:**

3   Hajar El Othmani,[1,2] Yangang Ren,[1] Abdelwahid Mellouki,[1] Véronique Daële,[1] Max R.

4   McGillen[1]*

5   [1] Institut de Combustion Aérothermique Réactivité et Environnement/OSUC−CNRS, 45071

6   Orléans, Cedex 2, France

7   [2] Faculty of Science, Mohammed V University in Rabat, 10100 Rabat, Morocco

8   * corresponding author, email: max.mcgillen@cnrs-orleans.fr

9   **Target journal:**

10   *Chemical Physics Letters*

11   **Abstract:**

12   Absolute measurements of the rate coefficient of the title reaction are reported from 251–373

13   K using the laser-induced fluorescence–pulsed-laser photolysis technique, together with

14   room-temperature relative rate determinations using a simulation chamber. These are the first

15   reported values of this rate coefficient, which demonstrates a predominantly negative

16   temperature dependence that is more pronounced than with other epoxides, suggesting that

17   pre-reactive complexes contribute to the overall reactivity, and that these complexes are

18   comparatively stable for OH + cyclohexene oxide, which may result from its bicyclic

19   structure. This work provides new insights into the lesser-studied reactivity of the epoxide

20   functionality.

21   **Keywords:** epoxide, oxirane, hydroxyl, atmospheric chemistry, kinetics, rate constant

22

23   **1. Introduction**

24

25   There are many sources of epoxides in Earth's atmosphere, both natural and anthropogenic.

26   Epoxides can be formed in the troposphere, mainly through the oxidation of alkenes. Some

27   epoxides are generated directly, from the reactions of alkenes with O_3 [1], NO_3 [2] and $O(^3P)$

28   [3]. Whereas others can arise from the ring closure reactions of secondary radical species

29   formed from alkenes, such as the atmospherically important isoprene epoxydiols [4].

1

30 Epoxides may also be emitted directly to the atmosphere from floral scents [5], as well as

31 emissions being inferred from their various industrial applications [6].

32 Given the large global emission of olefinic precursor molecules, and the variety of these

33 unsaturated species, it is logical to expect that a large and diverse flux of epoxides enters the

34 atmosphere each year, and that knowledge of the atmospheric chemistry of epoxides is

35 required to understanding the total life-cycle of an alkene emission. Another potential source

36 of epoxides comes from the low-temperature combustion of hydrocarbons, which is known to

37 generate a variety of oxirane species [7].

38 Once they are released or formed in the troposphere, epoxides are expected to react with

39 radical species in the gas phase to form more oxidized species, or engage in acid-catalyzed

40 ring-opening reactions in the heterogeneous phase, forming low-volatility polyols [8]. The

41 competition between these processes will be defined by their respective reaction rates. At the

42 time of writing very few kinetic measurements are available for the oxidation of reactions of

43 epoxides with atmospheric oxidants such as OH or Cl [9], which limits our understanding of

44 the overall environmental fate of compounds possessing the epoxide functionality.

45 In this study, we report the rate coefficient of the following reaction over the temperature

46 range 251–373 K:

47

48 OH + cyclohexene oxide   →   products   (1)
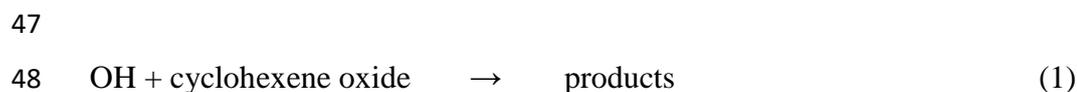
49

50 Cyclohexene oxide (1,2-epoxycyclohexane) is larger than those epoxides studied previously

51 [10–13], and, by virtue of the fact that it contains more C–H bonds than other epoxides found

52 in the kinetic database [9], is expected to react comparatively rapidly with OH and be lost

53 primarily through Reaction (1) under atmospheric conditions. The bicyclic structure of

54 cyclohexene oxide also contrasts with previously studied epoxides, and may influence its

55 reaction with OH. We will therefore discuss the reactivity of this molecule within the context

56 of other epoxides that have been studied so far.

2. Experimental methods

58 Two complementary methods were used in this work to determine the kinetics of Reaction

59 (1). First, an absolute measurement, employing the pulsed-laser photolysis–laser-induced

60 fluorescence (PLP–LIF) technique to measure the rate coefficient as a function of

61 temperature. Second, a relative rate chamber method was used to measure the rate coefficient

62   at room temperature. The details of these measurements are described in the following

63   subsections.

2.1 Absolute measurements using the PLP–LIF

65   The PLP–LIF apparatus used in this work has been used in several previous studies, and will

66   be described only briefly here, for more details, please see these earlier publications [14,15].

67   The LIF reactor is a jacketed 200 cm^3 Pyrex cell, with 4 quartz windows orthogonal to each

68   other. Heated/ cooled thermal transfer fluid (water or ethanol) was circulated through the outer

69   jacket in order to control the temperature of the gases inside the cell between 251 and 373 K.

70   Bath gas (He) pressures of ~100 Torr were used in all measurements, and were performed under

71   pseudo-first-order conditions such that [cyclohexene oxide] >> [OH]. OH radicals were

72   generated from the photolysis of precursor molecules using a 248 nm excimer laser operated at

73   10 Hz. To check for possible secondary interferences on OH decay profiles, two OH precursors

74   were used, H_2O_2 and HNO_3, which form OH through the following reactions:

75   H_2O_2 + hv →   2OH   (2)

76   HNO_3 + hv → $OH + NO_2$ (3)
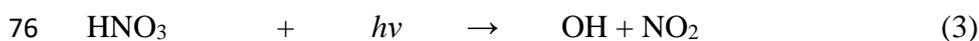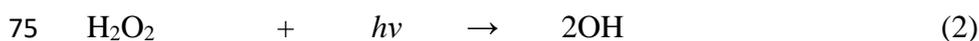
77   Both of these precursors were introduced by sweeping over the headspace/ bubbling of liquid

78   samples with carrier gas (He). Given that both of these precursors have poor transmission

79   through mass flow controllers (MFCs), the flow of these precursors was controlled upstream

80   of the sample using an MFC. This leads to an uncertainty in the exact OH precursor

81   concentration, which we estimate instead, similar to previous work [16], using the following

82   equation:

83   [OH precursor] $= k_d/k(T)_{OH}$

84   where k_d represents the decay of OH in the absence of the cyclohexene oxide co-reactant, and

85    $k(T)_{OH}$ is the temperature-dependent reaction rate of OH with the OH precursor molecule in

86   question.

87   OH radicals were probed at 10 Hz using a frequency-doubled Nd:YAG pumped dye laser

88   tuned to the $A^2\Sigma^+$ ($v = 1$) ← $X^2\Pi$ ($v = 0$) transition near 282 nm. The resultant 308 nm

89   fluorescence was detected with a photomultiplier tube equipped with a bandpass filter

90   centered around 310 nm.

91   OH temporal decays were generated by varying the delay time between the photolysis and

92   probe pulses, thus changing the reaction time between OH and cyclohexene oxide. These

93 decays were found to abide by pseudo-first-order kinetics in each case, as described in the

94 following equation:

95 $$\ln\left(\frac{[OH]_t}{[OH]_0}\right) = \ln\left(\frac{S_t}{S_0}\right) = -(k[\text{cyclohexene oxide}] + k_d)t = -k't$$

96 where the concentrations of OH, [OH], are proportional to fluorescence signal, S, at times 0

97 and t, respectively; and k' and k_d are first-order decay rates in the presence of and absence of

98 co-reactant cyclohexene oxide. k_d represents the decay of OH as a consequence of reactions

99 with OH precursors and diffusion out of the reaction volume, and was found to be exponential

100 over typical reaction times of 10,000 μs, and ranged from ~70–500 s^{-1} in our experiments. k'

101 ranged from ~3000–50,000 s^{-1}, and was likewise found to be exponential under the

102 experimental conditions of this study. Rate coefficients, k, were determined from a weighted

103 linear least-squares fit to k' against [cyclohexene oxide].

104 To minimize experiment errors associated with co-reactant concentration, [cyclohexene

105 oxide] was monitored on-line using a multipass FTIR spectrometer, that was positioned

106 directly downstream of the LIF reactor. To be quantitative, the integrated band intensity was

107 determined as part of this work, and the band located between 2800 and 3100 cm^{-1} with an

108 integrated band intensity of 3.66×10^{-17} cm molecule^{-1} was used in our analyses (see Figures

109 S1 and S2 for further details).

2.2 Relative measurements using a chamber apparatus

111 To complement the absolute measurements, a simulation chamber was used as an independent

112 determination of the rate coefficient of Reaction (1). This system consists of a large PTFE

113 Teflon chamber equipped with *in situ* multipass FTIR and high-resolution time-of-flight

114 proton-transfer reaction mass spectrometry (PTR-ToF-MS) measurements. This apparatus has

115 been employed recently to measure the reaction rates of compounds of low volatility [17], and

116 is therefore considered to be a good additional test of kinetic determinations for potentially

117 surface-active chemicals such as an epoxide, that may be affected by the higher surface

118 area:volume ratios – as well as higher reactant and OH precursor concentrations –

119 encountered in the LIF reactor and its accompanying FTIR cell.

120 Measurements were conducted at 295±2 K, in an atmosphere of purified air in a 7.3 m^3

121 cuboidal chamber constructed of Teflon foil, described in detail elsewhere [18]. OH radicals

122 were generated from methylnitrite, photolyzed at 365 nm using $24 \times$ UV-A T-40 L Viber-

123 Lourmat lamps in the following sequence of reactions:

124	CH$_3$ONO	+	hv	→	CH$_3$O + NO	(4)
125	CH$_3$O	+	O$_2$	→	CH$_2$O + HO$_2$	(5)
126	HO$_2$	+	NO	→	OH + NO$_2$	(6)
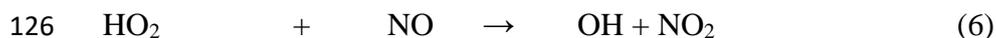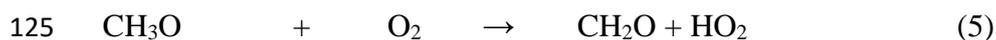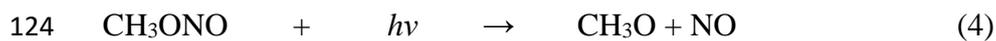
127 A relative method was employed to determine the rate coefficient, by measuring the decay

128 rate of [cyclohexene oxide] relative to that of a reference compound (1-propanol) with a

129 known OH rate coefficient, $k_{reference}$. Comparison of these decays, taking into account dilution

130 rate and wall-losses, k_d, yields the rate coefficient, k, through the following equation:

131 $$\ln\left(\frac{[\text{cyclohexene oxide}]_0}{[\text{cyclohexene oxide}]_t}\right) - k_d t = \frac{k_{\text{cyclohexene oxide}}}{k_{\text{reference}}} \ln\left(\frac{[\text{reference}]_0}{[\text{reference}]_t}\right) - k_d t$$

132 **2.3 Materials**

133 Cyclohexene oxide (>98%, Aldrich) was passed through several freeze-pump-thaw cycles

134 prior to use. Helium carrier gas (Alphagaz 2, Air Liquide, 99.999%) was used as supplied in

135 the PLP-LIF experiments. H$_2$O$_2$ (50 wt%, Alrich) was purified over the course of weeks with

136 a slow flow of purified air. Gas-phase HNO$_3$ was taken from the headspace of a sample of

137 70% redistilled HNO$_3$, dehydrated by the dropwise addition of pure H$_2$SO$_4$ in a HNO$_3$:H$_2$SO$_4$

138 ratio of 1:2 by volume, and maintained at 0°C in an ice bath. Methylnitrite was synthesized by

139 dropwise addition of 50% H$_2$SO$_4$ in water into a stirred saturated solution of NaNO$_2$ in

140 methanol, maintained at 0°C, the gaseous methylnitrite was then carried through a water

141 bubbler and a u-tube containing P$_2$O$_5$ using a slow flow of nitrogen, and cold trapped at -

142 196°C. 1- propanol (>99%, Aldrich) was used as supplied.

143 **3. Results and discussion**

144 Absolute measurements of the rate coefficient of Reaction (1) were measured using the PLP–

145 LIF apparatus between 251 and 373 K in 100 Torr (He). Second-order plots of k' against

146 [cyclohexene oxide] were of good quality in each case, with 2σ statistical errors between 2

147 and 7%. An example of one of these plots is shown in Figure 1, and a summary of rate

148 coefficient measurements together with experimental conditions is provided in Table S1.

149 Total combined estimated uncertainties including cyclohexene oxide concentration (5%),

150 pressure (2%) and temperature (2%) varied from 7–15%.
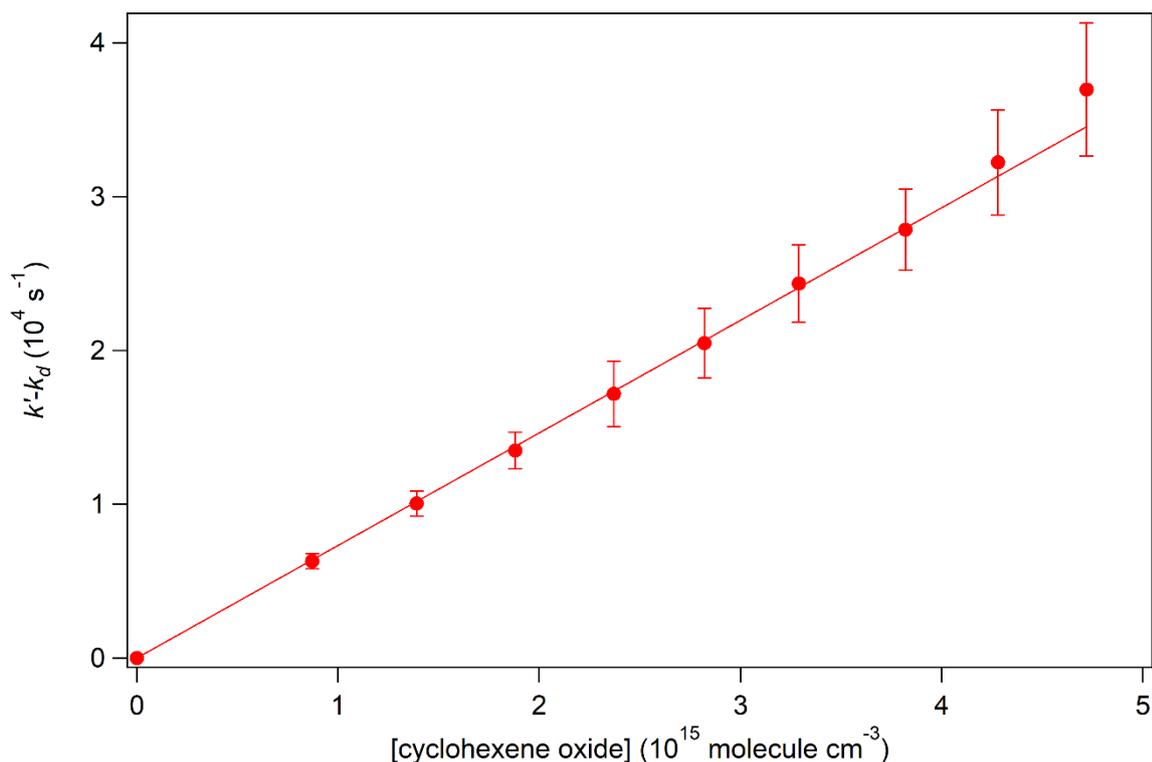
Figure 1: An example of a second-order plot measured at 274 K and 100 Torr (He). Bimolecular rate coefficients are obtained from the slopes of error-weighted linear least-squares fits to data such as these.

The relative rate measurements at 295 K in an atmosphere of purified air using 1-propanol as a reference generated relative rate plots of high linearity and negligible intercept as shown in Figure 2. We made two separate determinations in this way, which were found to be self-consistent and also in excellent agreement with our absolute measurements. The consistency between the chamber and PLP–LIF measurements suggests that there is no strong pressure or bath gas dependence under our experimental conditions. Relative rate coefficient determinations are tabulated in Table S2. Total combined uncertainties for relative measurements were dominated by the absolute uncertainties in the 1-propanol reference rate coefficient, which is 5.86×10^{-12} cm^3 molecule^{-1} s^{-1} at room temperature, with estimated uncertainties of 10% [9].
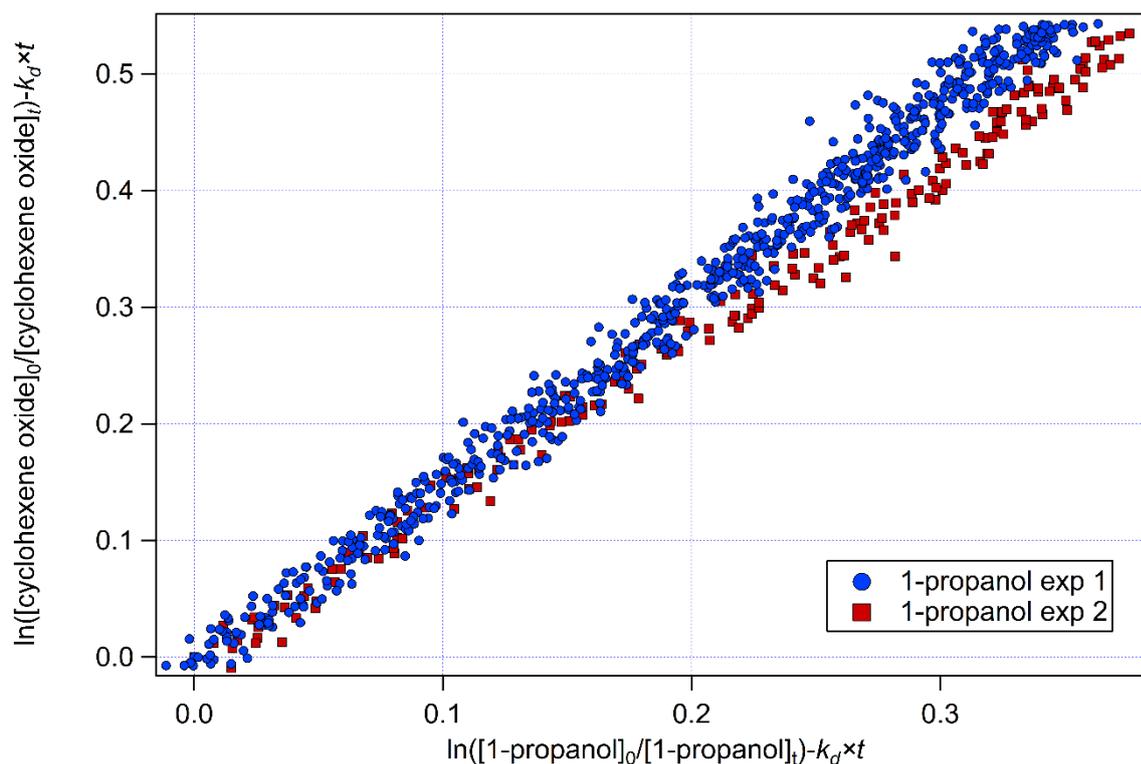
Figure 2: Relative rate experiments performed in a 7.3 m^3 chamber, in which the decay of cyclohexene oxide is monitored using a PTR-ToF-MS alongside the reference compound, 1-propanol. Experiments 1 and 2 correspond to rate coefficient determinations of 7.01±0.70 and 6.79±0.70 cm^3 molecule^{-1} s^{-1} respectively.

There are no measurements available in the literature with which we can compare our current data, and the only gas-phase rate coefficient data for cyclohexene oxide known to this study is the reaction with atomic chlorine [19].

An Arrhenius diagram showing the dependence of the rate coefficient of Reaction (1) upon temperature is shown in Figure 3. A negative temperature dependence is observed, with some minor curvature towards the higher temperatures of this study.
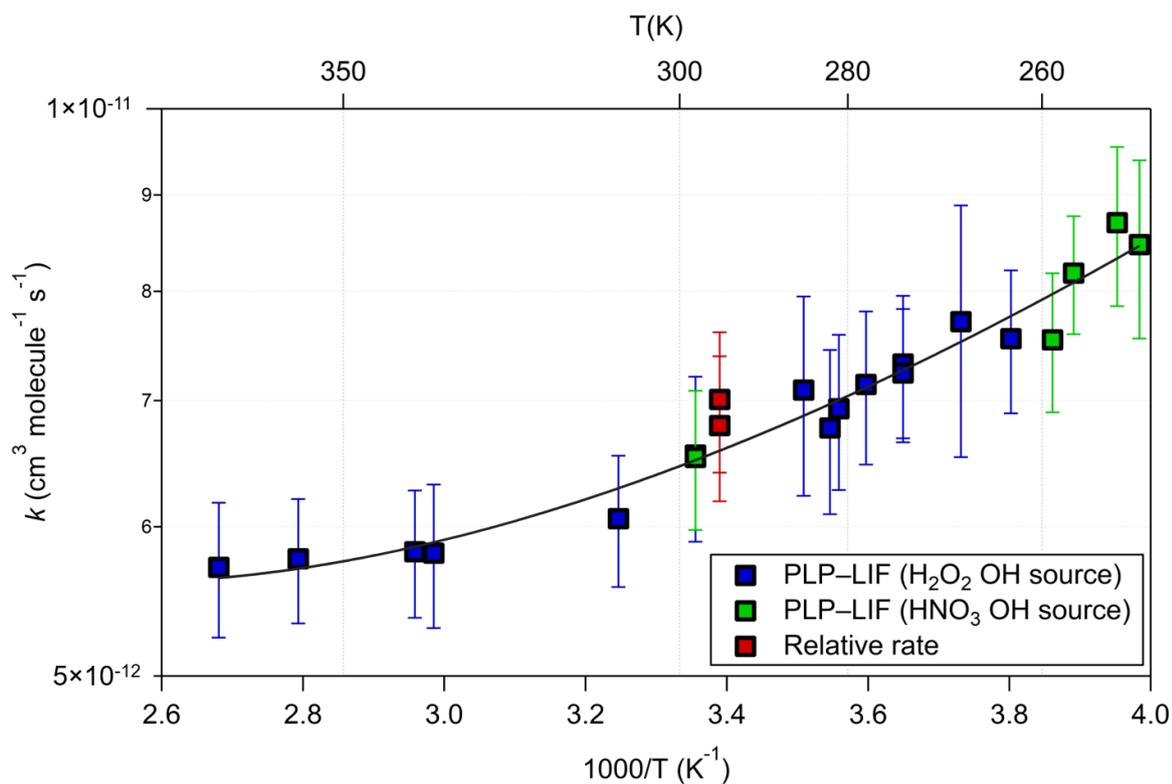
Figure 3: Arrhenius diagram showing the temperature dependence of the rate coefficient of OH + cyclohexene oxide. Error bars represent the total combined uncertainties. The black line represents a modified Arrhenius fit to the data.

A modified Arrhenius expression was found to fit the data adequately over the temperature range of 251–373 K:

$$k_1 = 7.20 \times 10^{-14} \exp\left(\frac{1349}{T}\right)\left(\frac{T}{300}\right)^{3.4}$$

These results are qualitatively consistent with the reactions of OH with other epoxides as well as with other oxygenates, which tend to exhibit curvature and/ or negative temperature dependence below room temperature. This suggests, as discussed in case of 1,2-epoxybutane, that pre-reactive complexes may be facilitating these reactions at low temperatures [13]. What remains uncertain is to what extent these complexes enhance the overall rate coefficient when compared with the direct hydrogen abstraction mechanisms that are available to these molecules. To guide this discussion, we present the temperature dependence of a variety of epoxides together with their alkane analogs in Figure 4. From this diagram, it is apparent that for much of the atmospheric temperature range, epoxides tend to be less reactive than their corresponding alkane structure. As discussed by El Othmani et al. (2021) [13], this reduction

193 in reactivity is likely to relate to the increased bond dissociation energy of C–H bonds
194 adjacent to the epoxide moiety. However, at lower temperatures, the OH rate coefficient of an
195 epoxide can be larger than that of its alkane analog. This phenomenon can be explained by the
196 increased stability of hydrogen-bonded van der Waals (vdW) complexes, which in turn
197 increases the probability of quantum tunnelling in these reactions, as has been observed for
198 other oxygenated molecules [20]. Besides this, there are other possibilities, such as the
199 existence of a submerged barrier, a low barrier, or a barrierless reaction towards products. In
200 such circumstances, quantum tunnelling may not contribute to the overall rate coefficient.
201 Submerged and low barriers are encountered frequently under atmospheric conditions such as
202 the electrophilic addition of OH to alkenes [21]. Low barriers are also observed in certain
203 hydrogen abstraction reactions, especially where weak C–H bonds are present, as is the case
204 of the reaction of OH + formaldehyde [22]. However, given that this is considered to be a
205 hydrogen abstraction mechanism, and accounting for the fact that the presence of the oxirane
206 functionality is calculated to increase bond strength in neighbouring C–H bonds [23], we
207 favour the hypothesis that vdW complexes are enhancing the overall rate coefficient at low
208 temperatures through quantum tunnelling.

209
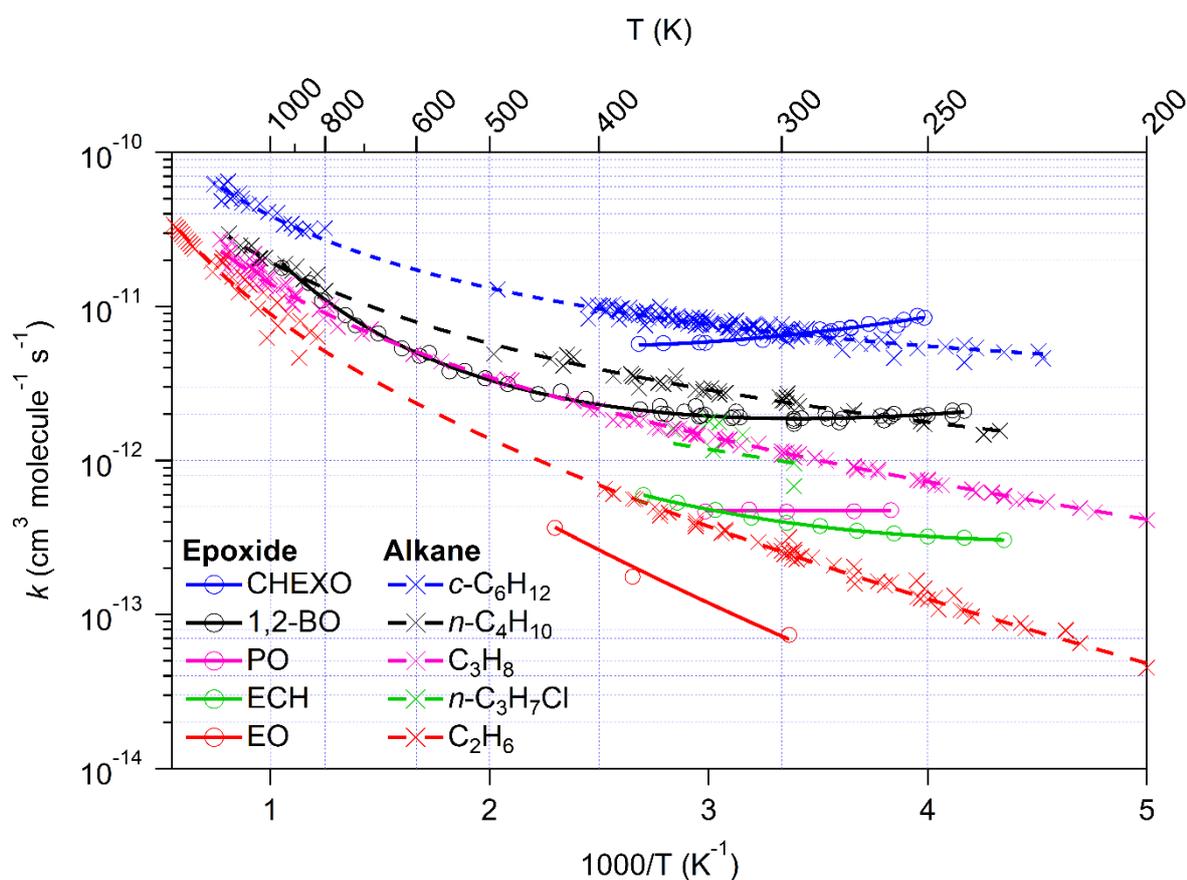
Figure 4: A comparison between the temperature dependences of epoxides and their alkane analogs. Epoxides are abbreviated as follows: CHEXO (cyclohexene oxide), 1,2-BO (1,2-butylene oxide), PO (propylene oxide), ECH (epichlorohydrin), EO (ethylene oxide). All kinetic data are taken from the database of McGillen et al. (2020) [9], except for the recent data of El Othmani et al. [13].

The temperature at which the rate coefficient of the epoxide overtakes its alkane counterpart – after some necessary extrapolation – appears to follow the order cyclohexene oxide > 1,2-epoxybutane > propylene oxide > epichlorohydrin > ethylene oxide. This also follows the order of decrease in the number of C–H bonds contained within each of these pairs. Simultaneously, it can be seen that the proportion by which the rate coefficient is decreased becomes less as the number of C–H bonds increases. This is intuitive, since the fraction of C–H bonds adjacent to the epoxide (i.e. the least reactive sites) decreases as the total number of C–H bonds grows, with the corollary being that, for larger epoxides, the reactivity would tend towards that of the alkane analog.

Assuming that our hypothesis is valid, and that the overall rate coefficient is affected by quantum tunnelling effects brought about by vdW complexes, the lifetime of the vdW complex will affect the extent to which the rate coefficient is enhanced by tunnelling processes. This lifetime increases as temperature (and kinetic energy) decreases. However, there are several other factors that can influence this phenomenon. One example is the binding energy of the complex, which will be largely dictated by the facility with which a molecule forms hydrogen bonds with the OH radical co-reactant. Carboxylic acids, for example, form particularly stable complexes, which reside in a potential energy well of ~33 kJ mol^{-1} [24], and as a result, their OH rate coefficients tend to be large, with a pronounced negative temperature dependence even at high temperatures [25]. A second factor is the entropic cost of forming the vdW complexes. These tend to have a cyclic structure, and as a consequence, have the capacity to shut down free rotors within molecules, which has been calculated to affect the phenomenological rate coefficient under some conditions [26]. Cyclohexene oxide is an interesting counterexample, in that it is purely cyclic to begin with, which should make the formation of the vdW complex more favourable energetically, a second factor contributing to this phenomenon is that the oxirane cycle is expected to be out-of-plane of the C_6 cycle, which may facilitate the participation of the neighbouring CH_2 group in a vdW complex. Both of which represent potential reasons why the onset of negative temperature dependence occurs at a higher temperature for Reaction (1) than with other epoxides. A further effect may

243   come from an increase in the rate of vibrational relaxion that is afforded to molecules of a

244   larger size, which would explain why the reaction of OH with ethylene oxide shows no

245   negative temperature dependence within the temperature range that it has been studied so far

246   [10].

247   Other interpretations of the overall u-shaped Arrhenius profiles of the epoxides are possible,

248   for example, this would be anticipated from modified transition state theory in systems with

249   negative activation energies [27]. However, in the absence of high-level calculations, we

250   cannot assess whether or not this is a better explanation of our kinetic results compared with

251   the statistical complexes mentioned above.

252   **4. Conclusions**

253   We present the first reported absolute kinetic measurements of the gas-phase reaction of OH +

254   cyclohexene oxide as a function of temperature between 251 and 373 K. This work serves to

255   extend the overall knowledge on the reactivity of epoxides towards the OH radical. Our

256   results indicate that the presence of the epoxide moiety in cyclohexene oxide leads to an

257   enhancement of the rate coefficient compared with its alkane analog, cyclohexane. This

258   suggests that the dominant loss process for this epoxide will be with atmospheric oxidants

259   such as the OH radical, and that acid-catalyzed ring-opening reactions for larger, more

260   reactive epoxides such as this may be of less importance. Assuming a representative

261   tropospheric OH concentration of 2×10^6 molecule cm^{-3}, and a room temperature rate

262   coefficient for Reaction (1) of 6.51×10^{-12} cm^3 molecule^{-1} s^{-1}, we estimate from the following

263   equation:

264    $$\tau = \frac{1}{k[\text{OH}]}$$

265   that the tropospheric lifetime, τ, of cyclohexene oxide is approximately 1 day. As it becomes

266   oxidized, this bicyclic molecule is expected (by analogy to the atmospheric fate of cyclohexyl

267   peroxy/ cyclohexyl alkoxy radicals) to lead to ring-opened products [28]. These have an

268   increased capacity for forming multifunctional oxygenated species, which we expect can

269   contribute to secondary organic aerosol formation.

References:

277 [1] R. Atkinson, S.M. Aschmann, J. Arey, E.C. Tuazon, Formation yields of epoxides and

278     $O(^3P)$ atoms from the gas-phase reactions of O_3 with a series of alkenes, Int. J. Chem.

279   Kinet. 26 (1994) 945–950. https://doi.org/10.1002/kin.550260908.

280 [2] I. Wängberg, I. Barnes, K.H. Becker, Product and Mechanistic Study of the Reaction of

281   NO_3 Radicals with α-Pinene, Environ. Sci. Technol. 31 (1997) 2130–2135.

282   https://doi.org/10.1021/es960958n.

283 [3] R.J. Cvetanović, Molecular Rearrangements in the Reactions of Oxygen Atoms with

284   Olefins, Can. J. Chem. 36 (1958) 623–634. https://doi.org/10.1139/v58-088.

285 [4] F. Paulot, J.D. Crounse, H.G. Kjaergaard, A. Kurten, J.M. St. Clair, J.H. Seinfeld, P.O.

286   Wennberg, Unexpected Epoxide Formation in the Gas-Phase Photooxidation of

287   Isoprene, Science. 325 (2009) 730–733. https://doi.org/10.1126/science.1172910.

288 [5] J.T. Knudsen, R. Eriksson, J. Gershenzon, B. Ståhl, Diversity and Distribution of Floral

289   Scent, Bot. Rev. 72 (2006) 1–120. https://doi.org/10.1663/0006-

290   8101(2006)72[1:DADOFS]2.0.CO;2.

291 [6] H.Q. Pham, M.J. Marks, Epoxy Resins, in: Wiley-VCH Verlag GmbH & Co. KGaA (Ed.),

292   Ullmanns Encycl. Ind. Chem., Wiley-VCH Verlag GmbH & Co. KGaA, Weinheim,

293   Germany, 2005: p. a09_547.pub2. https://doi.org/10.1002/14356007.a09_547.pub2.

294 [7] M.G. Christianson, A.C. Doner, M.M. Davis, A.L. Koritzke, J.M. Turney, H.F. Schaefer, L.

295   Sheps, D.L. Osborn, C.A. Taatjes, B. Rotavera, Reaction mechanisms of a cyclic ether

296   intermediate: Ethyloxirane, Int. J. Chem. Kinet. 53 (2021) 43–59.

297   https://doi.org/10.1002/kin.21423.

298 [8] E.C. Minerath, M.J. Elrod, Assessing the Potential for Diol and Hydroxy Sulfate Ester

299   Formation from the Reaction of Epoxides in Tropospheric Aerosols, Environ. Sci.

300   Technol. 43 (2009) 1386–1392. https://doi.org/10.1021/es8029076.

301 [9] M.R. McGillen, W.P.L. Carter, A. Mellouki, J.J. Orlando, B. Picquet-Varrault, T.J.

302   Wallington, Database for the kinetics of the gas-phase atmospheric reactions of organic

303   compounds, Earth Syst. Sci. Data. 12 (2020) 1203–1216. https://doi.org/10.5194/essd-

304   12-1203-2020.

305 [10] K. Lorenz, R. Zellner, Rate Constants and Vinoxy Product Yield in the Reaction OH +

306   Ethylene Oxide, Berichte Bunsenges. Für Phys. Chem. 88 (1984) 1228–1231.

307   https://doi.org/10.1002/bbpc.198400053.

308 [11] V.L. Orkin, V.G. Khamaganov, S.N. Kozlov, M.J. Kurylo, Measurements of Rate Constants

309   for the OH Reactions with Bromoform ($CHBr_3$), $CHBr_2Cl$, $CHBrCl_2$, and Epichlorohydrin

310   (C_3H_5ClO), J. Phys. Chem. A. 117 (2013) 3809–3818. https://doi.org/10.1021/jp3128753.

311 [12] A. Virmani, M.P. Walavalkar, A. Sharma, S. Sengupta, A. Saha, A. Kumar, Kinetic studies

312   of the gas phase reaction of 1,2-propylene oxide with the OH radical over a

313   temperature range of 261–335 K, Atmos. Environ. 237 (2020) 117709.

314   https://doi.org/10.1016/j.atmosenv.2020.117709.

315 [13] H. El Othmani, Y. Ren, Y. Bedjanian, S. El Hajjaji, C. Tovar, P. Wiesen, A. Mellouki, M.R.

316   McGillen, V. Daële, Gas-Phase Rate Coefficient of OH + 1,2-Epoxybutane Determined

317 between 220 and 950 K, ACS Earth Space Chem. (2021) acsearthspacechem.1c00050.
318 https://doi.org/10.1021/acsearthspacechem.1c00050.

319 [14] A. Mellouki, S. Téton, G. Laverdet, A. Quilgars, G. Le Bras, Kinetic studies of OH
320 reactions with H_2O_2, C_3H_8 and CH_4 using the pulsed laser photolysis - laser induced
321 fluorescence method, J. Chim. Phys. 91 (1994) 473–487.
322 https://doi.org/10.1051/jcp/1994910473.

323 [15] Y. Ren, M. Cai, V. Daële, A. Mellouki, Rate coefficients for the reactions of OH radical
324 and ozone with a series of unsaturated esters, Atmos. Environ. 200 (2019) 243–253.
325 https://doi.org/10.1016/j.atmosenv.2018.12.017.

326 [16] M.R. McGillen, M. Baasandorj, J.B. Burkholder, Gas-Phase Rate Coefficients for the OH
327 + *n*-, *i*-, *s*-, and *t*-Butanol Reactions Measured Between 220 and 380 K: Non-Arrhenius
328 Behavior and Site-Specific Reactivity, J. Phys. Chem. A. 117 (2013) 4636–4656.
329 https://doi.org/10.1021/jp402702u.

330 [17] Y. Ren, M.R. McGillen, V. Daële, J. Casas, A. Mellouki, The fate of methyl salicylate in
331 the environment and its role as signal in multitrophic interactions, Sci. Total Environ.
332 749 (2020) 141406. https://doi.org/10.1016/j.scitotenv.2020.141406.

333 [18] F. Bernard, G. Eyglunent, V. Daële, A. Mellouki, Kinetics and Products of Gas-Phase
334 Reactions of Ozone with Methyl Methacrylate, Methyl Acrylate, and Ethyl Acrylate, J.
335 Phys. Chem. A. 114 (2010) 8376–8383. https://doi.org/10.1021/jp104451v.

336 [19] C.M. Tovar, A. Haack, I. Barnes, I.G. Bejan, P. Wiesen, Experimental and theoretical
337 study of the reactivity of a series of epoxides with chlorine atoms at 298 K, Phys. Chem.
338 Chem. Phys. 23 (2021) 5176–5186. https://doi.org/10.1039/D0CP06033J.

339 [20] D.E. Heard, Rapid Acceleration of Hydrogen Atom Abstraction Reactions of OH at Very
340 Low Temperatures through Weakly Bound Complexes and Tunneling, Acc. Chem. Res.
341 51 (2018) 2620–2627. https://doi.org/10.1021/acs.accounts.8b00304.

342 [21] J.P. Senosiain, S.J. Klippenstein, J.A. Miller, Reaction of Ethylene with Hydroxyl Radicals:
343 A Theoretical Study [†], J. Phys. Chem. A. 110 (2006) 6960–6970.
344 https://doi.org/10.1021/jp0566820.

345 [22] A. Zanchet, P. del Mazo, A. Aguado, O. Roncero, E. Jiménez, A. Canosa, M. Agúndez, J.
346 Cernicharo, Full dimensional potential energy surface and low temperature dynamics of
347 the $H_2CO + OH \rightarrow HCO + H_2O$ reaction, Phys. Chem. Chem. Phys. 20 (2018) 5415–
348 5426. https://doi.org/10.1039/C7CP05307J.

349 [23] P.C. St. John, Y. Guan, Y. Kim, B.D. Etz, S. Kim, R.S. Paton, Quantum chemical
350 calculations for over 200,000 organic radical species and 40,000 associated closed-shell
351 molecules, Sci. Data. 7 (2020) 244. https://doi.org/10.1038/s41597-020-00588-x.

352 [24] J. Mendes, C.-W. Zhou, H.J. Curran, Theoretical Chemical Kinetic Study of the H-Atom
353 Abstraction Reactions from Aldehydes and Acids by Ḣ Atoms and ȮH, HȮ$_2$, and ĊH$_3$
354 Radicals, J. Phys. Chem. A. 118 (2014) 12089–12104.
355 https://doi.org/10.1021/jp5072814.

356 [25] V.G. Khamaganov, V.X. Bui, S.A. Carl, J. Peeters, Absolute Rate Coefficient of the OH +
357 $CH_3C(O)OH$ Reaction at T = 287−802 K. The Two Faces of Pre-reactive H-Bonding, J.
358 Phys. Chem. A. 110 (2006) 12852−12859. https://doi.org/10.1021/jp064922l.

359 [26] C.-W. Zhou, J.M. Simmie, H.J. Curran, Rate constants for hydrogen-abstraction by Ȯ H
360 from n-butanol, Combust. Flame. 158 (2011) 726–731.
361 https://doi.org/10.1016/j.combustflame.2010.11.002.

362 [27] L.N. Krasnoperov, J. Peng, P. Marshall, Modified Transition State Theory and Negative
363 Apparent Activation Energies of Simple Metathesis Reactions: Application to the

364 Reaction $CH_3 + HBr \rightarrow CH_4 + Br^\dagger$, J. Phys. Chem. A. 110 (2006) 3110–3120.
365 https://doi.org/10.1021/jp054435q.
366 [28] J. Platz, J. Sehested, O.J. Nielsen, T.J. Wallington, Atmospheric Chemistry of
367 Cyclohexane: UV Spectra of $c\text{-}C_6H_{11}{}^\bullet$ and $(c\text{-}C_6H_{11})O_2{}^\bullet$ Radicals, Kinetics of the Reactions
368 of $(c\text{-}C_6H_{11})O_2{}^\bullet$ Radicals with NO and NO_2, and the Fate of the Alkoxy Radical $(c\text{-}$
369 $C_6H_{11})O^\bullet$, J. Phys. Chem. A. 103 (1999) 2688–2695. https://doi.org/10.1021/jp984195x.
370